Mechanics of Microtubule Buckling Supported by Cytoplasm

Hanqing Jiang
e-mail: hanqing.jiang@asu.edu

Jiaping Zhang

Department of Mechanical and Aerospace Engineering, Arizona State University, Tempe, AZ 85287

The cytoskeleton provides the mechanical scaffold and maintains the integrity of cells. It is usually believed that one type of cytoskeleton biopolymer, microtubules, bears compressive force. In vitro experiments found that isolated microtubules may form an Euler buckling pattern with a long-wavelength for very small compressive force. This, however, does not agree with in vivo experiments where microtubules buckle with a short-wavelength. In order to understand the structural role of microtubules in vivo, we developed mechanics models that study microtubule buckling supported by cytoplasm. The microtubule is modeled as a linearly elastic cylindrical tube while the cytoplasm is characterized by different types of materials, namely, viscous, elastic, or viscoelastic. The dynamic evolution equations, the fastest growth rate, the critical wavelength, and compressive force, as well as equilibrium buckling configurations are obtained. The ability for a cell to sustain compressive force does not solely rely on microtubules but is also supported by the elasticity of cytoplasm. With the support of the cytoplasm, an individual microtubule can sustain a compressive force on the order of 100 pN. The relatively stiff microtubules and compliant cytoplasm are combined to provide a scaffold for compressive force. [DOI: 10.1115/1.2966216]

1 Introduction

It is believed that the mechanical behavior of an eukaryotic cell is primarily governed by a network of filament systems called the cytoskeleton [1]. The cytoskeleton supports a large volume of cytoplasm as well as provides the mechanical scaffold and maintains the integrity of cells [1–3]. Many cellular functions such as gene expression, cell division, motility, signal transduction, wound healing, and apoptosis are mediated by the physical properties of cytoskeleton. There are three major filamentous biopolymers comprising the cytoskeleton: microtubules, actin filaments, and intermediate filaments. Each cytoskeleton filament has different atomic structures and therefore has distinct mechanical functions and properties. For example, a microtubule (Fig. 1(*a*)) is a long (up to 50 μm), hollow cylindrical tube with inner and outer diameters of 15.4 nm and 25 nm, respectively [1,4]. The tube wall is formed from a dimerization of globular proteins (α-β tubulins) with one guanosine triphosphate (GTP) or guanosine diphosphate (GDP) nucleotide. Under the right conditions, tubulin heterodimers will polymerize to form long chained protofilaments (Fig. 1(*b*)), which bind to GDP in a circular arrangement to form a microtubule [1].

Microtubules are the stiffest biopolymers in cytoskeleton, and their bending rigidity is about 100 times larger than that of actin filaments, and therefore it is believed that microtubules typically carry most of the compressive forces [5–9]. Such large aspect ratio (25 nm in diameter/50 μm in length), however, suggests that isolated microtubules will exhibit classic Euler buckling with a single long-wavelength buckling pattern, as shown in Fig. 2(*a*). Using the reported bending rigidity $E_{\mathrm{MT}}I=2\times10^{-23}$ N m^2 [10], the critical load for Euler buckling of a microtubule is $P^c=4\pi^2E_{\mathrm{MT}}I/L^2=0.3$ pN, where E_{MT} is Young's modulus of microtubules, I is the moment of inertia, and L(=50 μm) is the length of a microtubule. This critical load for buckling is even one order of magnitude smaller than the microtubule polymerization force ($\sim$4 pN) measured in vitro [11], which suggests that the microtubules *cannot* sustain compressive force because they would buckle at a very small critical force. Another contradiction is that the single long-wavelength buckling pattern (Fig. 2(*a*)) does not agree with the highly curved microtubules observed in living cells [11,12], as illustrated in Fig. 2(*b*).

In order to understand the structural role of microtubules in living cells, Brangwynne et al. [13] conducted experimental studies on microtubule buckling in vivo. They found that individual microtubules can bear compressive forces that are about 100 times greater in vivo than they can in vitro. In vivo, microtubules also buckle at short-wavelengths ($\lambda=3$ μm). The mechanism for short-wavelength buckling was qualitatively explained by the lateral mechanical reinforcement supported by the surrounding elastic cytoskeleton. This study shed light on the mechanical role of microtubules in living cells although precise mechanics analysis is still needed.

This paper presents a structured analysis of the quantitative mechanics of microtubule buckling. In order to investigate the effects of surrounding cytoplasm on the buckling of microtubules, the cytoplasm is modeled using three different types of materials: viscous, elastic, and viscoelastic. Each cytoplasm model displays unique yet important results. This paper is organized as follows. Section 2 describes the microtubule model that is applied for various cytoplasm models. The analyses of microtubule buckling on viscous, elastic, and viscoelastic cytoplasms are given in Secs. 3–5, respectively, along with the corresponding discussions. Section 6 summarizes the results and discusses the importance of this study to biological understanding of the structural role of microtubules

2 Microtubule Modeling

The microtubule is modeled as an elastic cylindrical tube with outer diameter D_o(=25 nm) and inner diameter D_i(=15.4 nm). The microtubule is embedded in a three-dimensional cytoplasm and subject to an axial compressive force $P(>0)$ that leads to microtubule buckling with a short-wavelength (Fig. 2(*b*)). The von Karman theory [14] is used to account for the finite rotation effect in the buckling analysis. The axial strain in the microtubule is

Contributed by the Applied Mechanics Division of ASME for publication in the JOURNAL OF APPLIED MECHANICS. Manuscript received December 20, 2007; final manuscript received May 22, 2008; published online August 21, 2008. Review conducted by Krishna Garikipati.

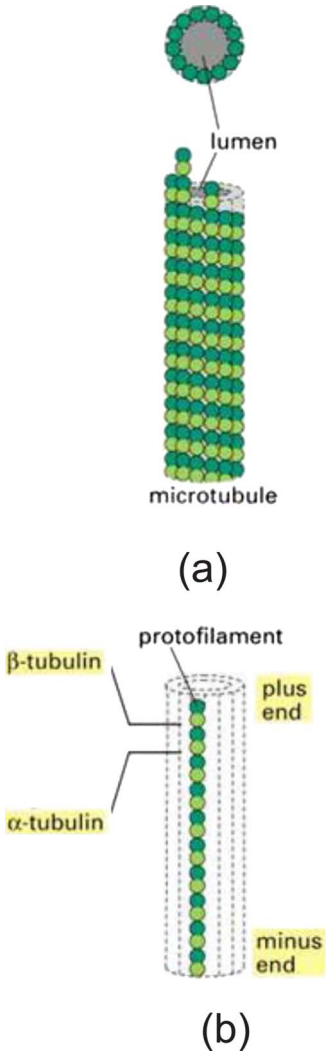

Fig. 1 The structure of a microtubule [1]. (*a*) The microtubule is a hollow cylindrical tube formed from 13 protofilaments aligned in parallel. (*b*) One protofilament consists of a string α-β heterodimers.

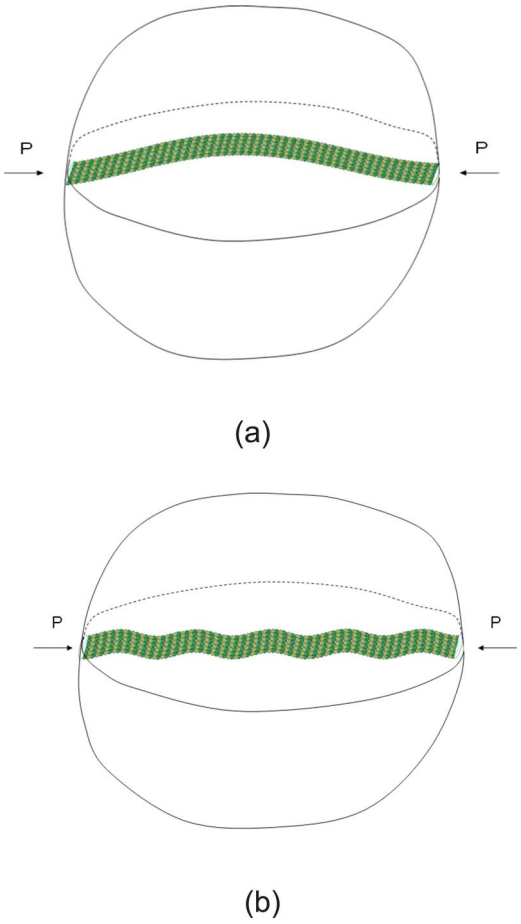

Fig. 2 (*a*) Microtubule buckles to a single long-wavelength pattern and (*b*) microtubule buckles to short-wavelength pattern

$$\varepsilon_{11} = \frac{\partial u_1}{\partial x_1} + \frac{1}{2}\left(\frac{\partial u_3}{\partial x_1}\right)^2 \tag{1}$$

where u_1 is the axial displacement and u_3 is the vertical displacement. The coordinate system is shown in Fig. 3, where x_1 is in the axial direction, x_2 is in the diameter direction, and x_3 is in the vertical direction. The linearly elastic constitutive model gives the axial force $N_{11}=E_{\mathrm{MT}}S\varepsilon_{11}$, where $S=\pi/4(D_o^2-D_i^2)$ is the cross-sectional area of the microtubule. The shear traction T_1 and normal traction T_3 at the microtubule/cytoplasm interface can be obtained from the equilibrium of forces [14]

$$T_1 = \frac{\partial N_{11}}{\partial x_1} \tag{2}$$

and

$$T_3 = E_{\mathrm{MT}} I \frac{\partial^4 u_3}{\partial x_1^4} - N_{11}\frac{\partial^2 u_3}{\partial x_1^2} - \frac{\partial N_{11}}{\partial x_1}\frac{\partial u_3}{\partial x_1} \tag{3}$$

where $I=\pi/64(D_o^4-D_i^4)$ is the moment of inertia of microtubules. The relatively stiff microtubule/compliant cytoplasm system has negligible shear stress at the interface, i.e., $T_1 \approx 0$ [15]. Equation (2) then gives constant axial force N_{11} and constant axial strain ε_{11}.

The buckling profile of the microtubule can be expressed as

$$u_3 = A\cos(kx_1) \tag{4}$$

where the multiple short-wavelength buckling pattern is assumed, the amplitude A and wave number k are to be determined, and $\lambda=2\pi/k$ is the buckling wavelength. The constant axial strain ε_{11} gives the axial displacement $u_1=kA^2\sin(2kx_1)/8$, where the condition $\int_0^{2\pi/k}(\partial u_1/\partial x_1)dx_1=0$ has been imposed to be consistent

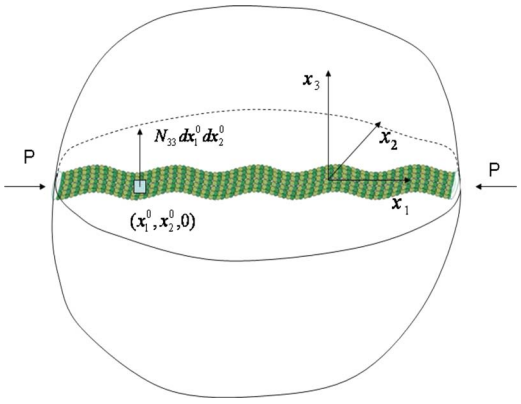

Fig. 3 The coordinate system used in the analysis

with the overall cytoplasm deformation [16]. Due to axial compressive force P, the axial strain then becomes

$$\varepsilon_{11} = \frac{1}{4}A^2k^2 - \frac{P}{E_{\mathrm{MT}}S} \tag{5}$$

and the vertical traction T_3 at the microtubule/cytoplasm interface is

$$T_3 = -\beta\cos(kx_1) \tag{6}$$

where

$$\beta = -E_{\mathrm{MT}}IAk^4 - E_{\mathrm{MT}}S\left(\frac{1}{4}A^2k^2 - \frac{P}{E_{\mathrm{MT}}S}\right)Ak^2 \tag{7}$$

For the buckling profile in Eq. (4), the bending energy per unit wavelength of the microtubule becomes

$$U_b = \frac{k}{2\pi}\int_0^{2\pi/k}\frac{1}{2}E_{\mathrm{MT}}I\left(\frac{\partial^2 u_3}{\partial x_1^2}\right)^2 dx_1 = \frac{1}{4}E_{\mathrm{MT}}Ik^4A^2 \tag{8}$$

The energy per unit wavelength due to axial strain is given by

$$U_a = \frac{1}{2}N_{11}\varepsilon_{11} = \frac{1}{2}E_{\mathrm{MT}}S\left(\frac{1}{4}A^2k^2 - \frac{P}{E_{\mathrm{MT}}S}\right)^2 \tag{9}$$

3 Microtubule Buckling on Viscous Cytoplasm

We first model the surrounding cytoplasm as a three-dimensional viscous flow since the major element of cytoplasm, cytosol, typically consists of fluid. Cytoplasmic streaming is such a three-dimensional viscous flow in the cells and surrounds the cytoskeleton [17]. The viscous cytoplasm is assumed to be incompressible, i.e.,

$$\nabla\cdot\dot{\mathbf{u}} = 0 \tag{10}$$

where $\dot{\mathbf{u}}$ is the velocity, i.e., $\dot{\mathbf{u}} = d\mathbf{u}/dt$; t is the time. Some biological experiments have shown that upon forces (e.g., centrifugal forces), the cytoplasmic streaming becomes steady on the time scale of minutes (e.g., Refs. [18,19]). Moreover, the biological study used measured values to estimate the Reynolds number and found that the Reynolds number Re is very low for cytoplasmic streaming, for instance, $Re < 10^{-3}$, as reported by Pickard [20]. With the conditions of steady state and low Reynolds number of cytoplasmic streaming that surrounds the cytoskeleton, we model the viscous cytoplasm as Stokes flow that is characterized by Stokes equation

$$-\nabla P + \eta\nabla^2\dot{\mathbf{u}} = 0 \tag{11}$$

where P is the pressure and h is the dynamic viscosity of cytoplasm. A vertical traction $-T_3 = \beta\cos(kx_1)$ (where T_3 is given in Eq. (6)) is applied over the area $[|x_2| \le R, x_3 = 0]$ where the microtubule contacts with the viscous cytoplasm. The traction $-T_3$ is assumed to be uniform over the diameter of the microtubule (but periodic in the x_1 direction), which gives the following stress traction in the x_3 direction within the three-dimensional viscous cytoplasm:

$$N_{33} = -\frac{T_3}{2R} = \frac{\beta}{2R}\cos(kx_1) \tag{12}$$

over the diameter $(2R = (D_i + D_o)/2)$ of the microtubules (Fig. 3).

Instead of solving this three-dimensional Stokes equation with stress traction N_{33} as a boundary condition for the area $[|x_2| \le R, x_3 = 0]$ and traction free for the other areas, we use the solution of flow due to a point force. We now consider the flow due to a unit point force at a point of $\mathbf{x}^0 = (x_1^0, x_2^0, 0)$ within the three-dimensional viscous cytoplasm. The Stokes equation with a singular point force term is then given by

$$-\nabla P + \eta\nabla^2\dot{\mathbf{u}} + \mathbf{e}_3\delta(\mathbf{x} - \mathbf{x}^0) = 0 \tag{13}$$

where $\mathbf{e}_3$ is the unit vector in the x_3 direction and δ is the Dirac delta function. Using the Stokes stream function method, the flow due to a point force can be resolved and the details were given by Pozrikidis [21]. The vertical velocity $\dot{u}_3$ at a point $\mathbf{x} = (x_1, x_2, 0)$ is given by $1/8\pi\eta\sqrt{(x_1 - x_1^0)^2 + (x_2 - x_2^0)^2}$. Then for the distributed stress traction N_{33} given by Eq. (12), the vertical velocity $\dot{u}_3$ at a point $\mathbf{x} = (x_1, x_2, 0)$ is the integration over the area covered by microtubule,

$$\begin{aligned}\dot{u}_3(x_1, x_2, 0) &= \int_{-R}^{R}\int_{-\infty}^{\infty}\frac{\beta\cos(kx_1^0)}{2R}\frac{1}{8\pi\eta} \\ &\quad\times\frac{1}{\sqrt{(x_1 - x_1^0)^2 + (x_2 - x_2^0)^2}}dx_1^0dx_2^0 \\ &= \int_{-R}^{R}\frac{\beta\cos(kx_1)}{8\pi R\eta}Y_0(k|x_2^0 - x_2|)dx_2^0\end{aligned} \tag{14}$$

where Y_0 is the modified Bessel function of the second kind [22]. Since the diameter of microtubules $R(=12.5\ \mathrm{nm})$ is much smaller than the observed buckling wavelength $\lambda(=3\ \mu\mathrm{m})$, then $k|x_2^0 - x_2| \le 2kR = 4\pi R/\lambda \ll 1$. The velocity in Eq. (14) then can be approximately expressed as

$$\begin{aligned}\dot{u}_3(x_1, x_2, 0) &= \int_{-R}^{R}\frac{\beta\cos(kx_1)}{8\pi R\eta}\left(\ln\frac{k|x_2^0 - x_2|}{2} + \gamma\right)dx_2^0 \\ &= \frac{\beta\cos(kx_1)}{8\pi R\eta}\{2R(1-\gamma) + 2R\ln 2 - (R + x_2)\ln[k(R \\ &\quad + x_2)] - (R - x_2)\ln[k(R - x_2)]\}\end{aligned} \tag{15}$$

where

$$\gamma = \lim_{n\to\infty}\left[\sum_{i=1}^{n}\frac{1}{i} - \ln(n)\right] = 0.577$$

is Euler's constant.

The viscous cytoplasm and the buckled microtubule are coupled through the continuity condition across the microtubule/cytoplasm interface. Specifically, the vertical velocity $\dot{u}_3$ of the viscous cytoplasm in Eq. (15) is continuous with the vertical velocity of the microtubule resulted from the displacement in Eq. (4) at the interface. We realize that the vertical velocity in Eq. (15) also depends on the x_2 direction so that this continuity is on the average sense, i.e., the average vertical velocity of the viscous cytoplasm over the diameter of the microtubule

$$\dot{u}_3^{\mathrm{avg}}(x_1) = \frac{1}{2R}\int_{-R}^{R}\dot{u}_3(x_1, x_2, 0)dx_2 = \frac{\beta\cos(kx_1)}{8\pi\eta}[3 - 2\gamma - 2\ln(kR)] \tag{16}$$

is the same as the vertical velocity of the microtubule from the displacement in Eq. (4). Thus the continuity condition is

$$\frac{dA}{dt} = \frac{\beta}{8\pi\eta}[3 - 2\gamma - 2\ln(kR)] \tag{17}$$

We consider that the microtubule buckling originated from the accumulation of small fluctuations, which consists of many small perturbation components with each component expressed as a sinusoidal form as in Eq. (4). For small perturbation with vertical displacement A, β in Eq. (7) is linearized by keeping the first-order terms of A,

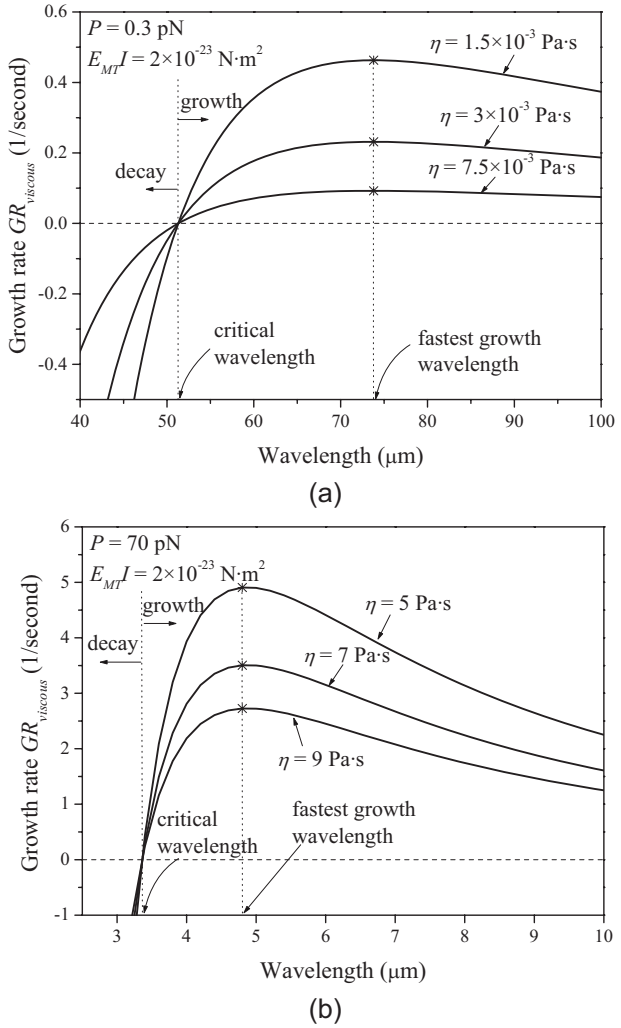

Fig. 4 The relationship of growth rate and wavelength for viscous cytoplasm. (*a*) Growth rate versus wavelength for small axial compressive force and (*b*) growth rate versus wavelength for large axial compressive force.

$$\beta = E_{\mathrm{MT}} I \left(\frac{P}{E_{\mathrm{MT}} I} - k^2 \right) k^2 A \tag{18}$$

The linear ordinary differential equation for small perturbation A then becomes

$$\frac{dA}{dt} = \frac{E_{\mathrm{MT}} I}{8\pi\eta} \left(\frac{P}{E_{\mathrm{MT}} I} - k^2 \right) [3 - 2\gamma - 2\ln(kR)] k^2 A \tag{19}$$

Let $A_0 = A(t=0)$ be the initial amplitude, the evolution of the vertical displacement is

$$A(t) = A_0 \exp\left\{ \frac{E_{\mathrm{MT}} I}{8\pi\eta} \left(\frac{P}{E_{\mathrm{MT}} I} - k^2 \right) [3 - 2\gamma - 2\ln(kR)] k^2 t \right\} = A_0 e^{\mathrm{GR}_{\mathrm{viscous}} t} \tag{20}$$

where

$$\mathrm{GR}_{\mathrm{viscous}} = \frac{E_{\mathrm{MT}} I}{8\pi\eta} \left(\frac{P}{E_{\mathrm{MT}} I} - k^2 \right) [3 - 2\gamma - 2\ln(kR)] k^2 \tag{21}$$

denotes the growth rate of the initial perturbation.

Figure 4 shows $\mathrm{GR}_{\mathrm{viscous}}$ versus wavelength for fixed bending rigidity $E_{\mathrm{MT}} I = 2 \times 10^{-23}$ N m^2 [10] and various axial compressive force P and viscosity η. Figure 4(*a*) gives the growth rate $\mathrm{GR}_{\mathrm{viscous}}$ and wavelength relationship for small compressive force ($P = 0.3$ pN) and low viscosity $\eta = 1.5 \times 10^{-3} - 7.5 \times 10^{-3}$ Pa s to model the fluid-phase cytosol that is only several times as viscous as water (e.g., Refs. [23–25]). When $\mathrm{GR}_{\mathrm{viscous}} > 0$ for certain wavelengths, the initial fluctuations characterized by these wavelengths grow in an exponential law (Eq. (20)), while when $\mathrm{GR}_{\mathrm{viscous}} < 0$ for some wavelengths, the initial fluctuations associated with these wavelengths decay and the microtubules remain straight. The critical condition $\mathrm{GR}_{\mathrm{viscous}} = 0$ gives the critical wavelength

$$\lambda^c_{\mathrm{viscous}} = 2\pi \sqrt{\frac{E_{\mathrm{MT}} I}{P}} \tag{22}$$

The critical wavelength $\lambda^c_{\mathrm{viscous}}$ does not depend on viscosity η and is 51.3 μm, shown in Fig. 4(*a*). The initial fluctuations with wavelengths greater than $\lambda^c_{\mathrm{viscous}}$ will grow; however, the fluctuations with wavelengths smaller than $\lambda^c_{\mathrm{viscous}}$ will decay. Equation (22) also indicates that no matter how small the force is, there exists a critical wavelength $\lambda^c_{\mathrm{viscous}}$ to ensure growth from initial fluctuations. In other words, dynamic growth is guaranteed to occur in viscous cytoplasm.

It is also noticed that the critical wavelength $\lambda^c_{\mathrm{viscous}}$ is identical to the critical length for Euler buckling, which suggests that a very small axial compressive force (on the order of 1 pN depending on the microtubule length) may lead to microtubule buckling with a large wavelength. However, the buckling of microtubules on viscous cytoplasm due to a small compressive force does not indicate that the microtubules cannot bear a compressive force. The growth or decay in this section is just the initial stage, while the compressive force that microtubule can sustain is determined by final equilibrium stage as to be discussed in Sec. 4.

Each curve in Fig. 4(*a*) has a maximum (marked by $*$ in Fig. 4(*a*)), which denotes the fastest growth rate. The corresponding fastest growth wavelength is determined by $\partial \mathrm{GR}_{\mathrm{viscous}} / \partial k = 0$,

$$\lambda = 2\pi \sqrt{\frac{E_{\mathrm{MT}} I}{2P} \frac{5 - 4\gamma - 4\ln(2\pi R/\lambda)}{1 - \gamma - \ln(2\pi R/\lambda)}} \tag{23}$$

Numerical results show that $5 - 4\gamma - 4\ln(2\pi R/\lambda) / 1 - \gamma - \ln(2\pi R/\lambda) \approx 4$ for all wavelengths, such that

$$\lambda^{\text{fastest growth}}_{\mathrm{viscous}} \approx 2\pi \sqrt{\frac{2E_{\mathrm{MT}} I}{P}} \tag{24}$$

Equation (24) clearly shows that the fastest growth wavelength is independent of viscous cytoplasm, while the corresponding fastest growth rate is inversely proportional to the viscosity. More importantly, the fastest growth rate is about 1/s, which suggests that the growth of initial fluctuation is on the order of seconds. This time scale agrees well with in vivo experiments of Brangwynne et al. [13].

Corresponding to the force generated by optical and magnetic tweezers, the growth rate $\mathrm{GR}_{\mathrm{viscous}}$ and wavelength relationship for cells due to a large compressive force ($P = 70$ pN) and moderate viscosity ($\eta = 5 - 9$ Pa s [25]) are shown in Fig. 4(*b*). Similar curves are shown and the critical and fastest growth wavelengths are 3.3 μm and 4.8 μm, respectively.

The study for viscous cytoplasm shows the following.

(1) Any small fluctuations that have wavelength greater than critical wavelength (Eq. (22)) will grow no matter how small the compressive force P is.
(2) Cytoplasm viscosity only affects the growth rate; the smaller the viscosity, the larger the growth rate; cytoplasm viscosity cannot determine the occurrence of the growth.
(3) Critical wavelength and fastest growth wavelength do not depend on viscosity.
(4) The compressive force that a microtubule can sustain before buckling is very small if the surrounding is a viscous cytoplasm.

It should be pointed out that the steadiness of cytoplasmic streaming and small perturbation (Eq. (20)) are two distinct concepts. The former indicates that the cytoplasmic streaming is steady upon external force/stress. While the latter, the small perturbation, evolves to respond to the steady cytoplasmic streaming, which is not steady, as shown in Eq. (20).

4 Microtubule Buckling on Elastic Cytoplasm

The elasticity of the cytoplasm originated from the cytoskeleton [26]. The elastic cytoplasm stores the deformation energy to stabilize the microtubules/cytoplasm system such that the equilibrium configuration (e.g., equilibrium wavelength) is determined by the energetics of the system. In this section, we study the final equilibrium stage by modeling the cytoplasm as a three-dimensional linearly elastic solid in this section. The shear modulus μ_e is used to characterize the incompressible elastic cytoplasm. The energetically favorable buckling pattern is determined using the energy method.

The three-dimensional elastic cytoplasm is subject to vertical traction $-T_3$ (where T_3 is given in Eq. (6)) within the area $[|x_2| \leq R, x_3=0]$. The normal traction $-T_3$ is assumed to be uniform over the microtubule diameter $2R$, which gives the nonvanishing stress traction in the x_3 direction $N_{33}=-T_3/2R=\beta\cos(kx_1)/2R$ the same as Eq. (12) in viscous analysis.

Based on Gaussian's divergence theorem, the strain energy per unit wavelength in the elastic cytoplasm is

$$U_s=\frac{k}{2\pi}\cdot\frac{1}{2}\int_V \boldsymbol{\sigma}:\boldsymbol{\varepsilon}dV=\frac{k}{4\pi}\int_{S_\sigma} N_{33}u_3^{\text{cytoplasm}}dS$$
$$=\frac{k}{4\pi}\int_{-R}^{R}\int_0^{2\pi/k} N_{33}u_3^{\text{cytoplasm}}dx_1dx_2 \tag{25}$$

where S_σ is the area $[|x_2|\leq R, x_3=0]$ where the microtubule contacts with the cytoplasm and $u_3^{\text{cytoplasm}}$ is the displacement on the area S_σ, which is obtained analytically from Kelvin's solution [27].

For a unit normal point force at $\mathbf{x}^0=(x_1^0,x_2^0,0)$ within a three-dimensional infinite elastic solid, Kelvin's solution gives the vertical displacement at the point $\mathbf{x}=(x_1,x_2,0)$ as $(1/8\pi\mu_e)1/\sqrt{(x_1-x_1^0)^2+(x_2-x_2^0)^2}$. For the distributed load N_{33}, the displacement at point $\mathbf{x}=(x_1,x_2,0)$ for elastic cytoplasm is the integration over the entire microtubule diameter $2R$,

$$u_3^{\text{cytoplasm}}(x_1,x_2,0)=\int_{-R}^{R}\int_{-\infty}^{\infty}\frac{\beta\cos(kx_1^0)}{16\pi R\mu_e}$$
$$\times\frac{1}{\sqrt{(x_1-x_1^0)^2+(x_2-x_2^0)^2}}dx_1^0dx_2^0$$
$$=\frac{\beta\cos(kx_1)}{8\pi R\mu_e}\{2R(1-\gamma)+2R\ln 2$$
$$-(R+x_2)\ln[k(R+x_2)]-(R-x_2)\ln[k(R-x_2)]\} \tag{26}$$

where the condition $R/\lambda\ll 1$ has been used. Because the microtubule/elastic cytoplasm interface is replaced by the normal traction in Eq. (6), the above displacement for the elastic cytoplasm is continuous with the displacement in Eq. (4) for the buckled microtubule only on the average sense.

The strain energy in the elastic cytoplasm is then obtained from Eqs. (25) and (26) as

$$U_s=\frac{k}{4\pi}\int_{x_2=-R}^{R}\int_{x_1=0}^{2\pi/k}\frac{\beta}{2R}\cos(kx_1)\frac{\beta\cos(kx_1)}{8\pi R\mu_e}\{2R(1-\gamma)+2R\ln 2$$
$$-(R+x_2)\ln[k(R+x_2)]-(R-x_2)\ln[k(R-x_2)]\}dx_1dx_2$$
$$=\frac{\beta^2}{32\pi\mu_e}[3-2\gamma-2\ln(kR)] \tag{27}$$

The total potential energy Π_{tot} of the system is the sum of bending energy (Eq. (8)) and axial strain energy (Eq. (9)) in the microtubule and the strain energy in the elastic cytoplasm (Eq. (27)). However, for the microtubule vertical displacement in Eq. (4) and the cytoplasm vertical displacement in Eq. (26), which are not continuous, the potential energy becomes

$$\Pi_{\text{tot}}=U_b+U_m+U_s-\int_{S_\sigma}\Lambda(u_3-u_3^{\text{cytoplasm}})dS \tag{28}$$

where Λ is the Lagrange multiplier. The variation of the above potential energy with respect to Λ requires $u_3=u_3^{\text{cytoplasm}}$ and the variation with respect to the displacement u_3 or $u_3^{\text{cytoplasm}}$ gives Λ to be the traction T_3 (Eq. (6)) at the interface. In the following the Lagrange multiplier Λ is replaced by the traction T_3 in Eq. (6). The potential energy is then obtained as

$$\Pi_{\text{tot}}=\frac{1}{2}E_{\text{MT}}S\left(\frac{1}{4}A^2k^2-\frac{P}{E_{\text{MT}}S}\right)^2+\frac{1}{4}E_{\text{MT}}Ik^4A^2+\frac{1}{2}\beta A-\frac{\beta^2}{32\pi\mu_e}[3$$
$$-2\gamma-2\ln(kR)] \tag{29}$$

which depends on buckling amplitude A and wavelength $\lambda=2\pi/k$.

The minimization of potential energy Π_{tot} in Eq. (29) with respect to the buckling amplitude A, $\partial\Pi_{\text{tot}}/\partial A=0$, gives

$$A=\begin{cases}\dfrac{2}{k}\sqrt{\dfrac{P-P^c_{\text{elastic}}}{E_{\text{MT}}S}}, & P\geq P^c_{\text{elastic}}\\ 0, & P<P^c_{\text{elastic}}\end{cases} \tag{30}$$

where

$$P^c_{\text{elastic}}=\frac{8\pi\mu_e}{k^2}\frac{1}{3-2\gamma-2\ln(kR)}+E_{\text{MT}}Ik^2 \tag{31}$$

is the critical compressive force for buckling. Equation (30) suggests that the buckling occurs only when the compressive force P reaches a critical force P^c_{elastic} given by Eq. (31), in which the wave number k is to be determined.

The minimization of potential energy with respect to the wave number, $\partial\Pi_{\text{tot}}/\partial k=0$, gives the following nonlinear equation for k:

$$k\left(\frac{E_{\text{MT}}I}{\mu_e}\right)^{1/4}=\left\{\frac{16\pi[1-\gamma-\ln(kR)]}{[3-2\gamma-2\ln(kR)]^2}\right\}^{1/4} \tag{32}$$

For reported microtubule bending rigidity $E_{\text{MT}}I=2\times10^{-23}$ N m^2 [10] and the wide range of shear modulus of the surrounding $\mu_e=1-1000$ Pa [28], the numerical results show that

$$k^c_{\text{elastic}}\approx\frac{5}{4}\left(\frac{\mu_e}{E_{\text{MT}}I}\right)^{1/4} \tag{33}$$

or equivalently,

$$\lambda^c_{\text{elastic}}=\frac{8\pi}{5}\left(\frac{E_{\text{MT}}I}{\mu_e}\right)^{1/4} \tag{34}$$

At this critical wavelength, the amplitude A is

$$A=\frac{8}{5}\left(\frac{E_{\text{MT}}I}{\mu_e}\right)^{1/4}\sqrt{\frac{P-P^c_{\text{elastic}}}{E_{\text{MT}}S}} \tag{35}$$

and the critical force P^c_{elastic} is

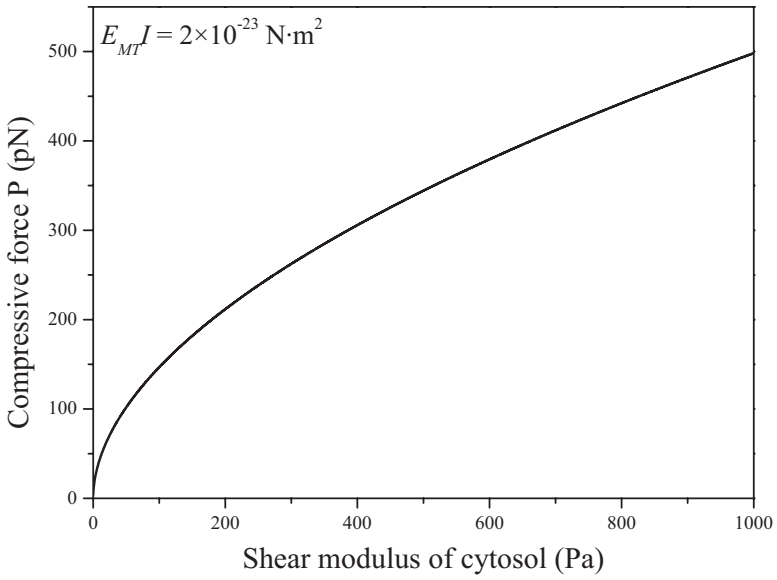

Fig. 5 The relationship between the compressive force *P* that an individual microtubule bears before buckling and the shear modulus of the elastic cytoplasm

$$P^c_{\text{elastic}} = \frac{25}{16}\sqrt{E_{\text{MT}}I\mu_e}\left\{1 + \frac{2048\pi}{625[3 - 2\gamma - 2\ln(2\pi R/\lambda^c_{\text{elastic}})]}\right\} \tag{36}$$

The buckling wavelength given by Eq. (34) is independent of axial compressive force P and solely determined by the ratio of shear modulus of the elastic cytoplasm and the bending rigidity of microtubules. Therefore, the buckling wavelength is an intrinsic property of microtubules/elastic cytoplasm systems and completely determined by their mechanical properties. Since the reported shear modulus μ_e of cytoplasm has extremely large scattering, ranging from 0.1 Pa to 1000 Pa [28], the buckling wavelength also exhibits large scattering. The smallest wavelength is about 1.9 μm while the largest wavelength is 19 μm. If a median value of μ_e=200 Pa is used, the present analysis gives 2.8 μm wavelength, which agrees very well with experiments of Brangwynne et al. [13].

The critical axial compressive force P^c_{elastic} to buckle microtubules (Eq. (36)) depends on both the bending rigidity of microtubules and the shear modulus of the cytoplasm. Therefore, the compressive force that an individual microtubule can bear depends on both the bending rigidity of microtubules and the shear modulus of cytoplasm as well. Figure 5 shows the relationship between the compressive force P that an individual microtubule sustains before buckling and the shear modulus of cytoplasm for a given bending rigidity of microtubules as $E_{\text{MT}}I=2\times10^{-23}$ N m^2 [10]. The results show that the compressive force is on the order of 100 pN, except when the shear modulus is less than 20 Pa. This study clearly indicates that the ability of a cell to bear compressive force depends on both microtubules and cytoplasm: The relatively stiff microtubules are combined with the compliant cytoplasm to sustain the compressive force.

The main findings for microtubule buckling on elastic cytoplasm are the following.

(1) The buckling wavelength does not depend on the axial force P but on the ratio of shear modulus of the elastic cytoplasm and bending rigidity of the microtubules.
(2) The compressive force is on the order of 100 pN for most cytoplasm with a shear modulus larger than 20 Pa.
(3) The ability to sustain compressive force is governed by both stiff microtubules and compliant cytoplasm.

5 Microtubule Buckling on Viscoelastic Cytoplasm

In this section, we study microtubule buckling supported by the viscoelastic cytoplasm. Cytoplasm exhibits both viscosity from fluid and elasticity from solid cytoskeleton networks, which has been shown in various experiments [29].

The surrounding cytoplasm that consists of fluid and cytoskeleton is modeled as an isotropic linearly viscoelastic material. The stress-strain relation is described in an integral form [30]

$$\boldsymbol{\sigma}(t) = 2\int_{-\infty}^{t}\mu(t-\tau)\frac{\partial\boldsymbol{\varepsilon}(\tau)}{\partial\tau}d\tau + \boldsymbol{\delta}\int_{-\infty}^{t}\lambda(t-\tau)\frac{\partial(\boldsymbol{\varepsilon}:\boldsymbol{\delta})}{\partial\tau}d\tau \tag{37}$$

where t is the time, $\mu(t)$ and $\lambda(t)$ are time-dependent relaxation moduli, and $\boldsymbol{\delta}$ is the second-order identity tensor. The equilibrium equation without body force and inertia term is $\nabla\cdot\boldsymbol{\sigma}=0$. The strain-displacement relation is linear, i.e., $\boldsymbol{\varepsilon}=(\nabla\mathbf{u}+\mathbf{u}\nabla)/2$. Within the three-dimensional viscoelastic cytoplasm, only the area $[|x_2|\leq R, x_3=0]$ that contacts with the buckled microtubule has prescribed traction $-T_3=\beta\cos(kx_1)$, where T_3 is given in Eq. (6). We also assume that the traction $-T_3$ is uniformly distributed over the diameter of microtubules, i.e., $N_{33}=-T_3/2R=\beta\cos(kx_1)/2R$ (Fig. 3). A boundary value problem for viscoelastic cytoplasm is then established.

This viscoelastic problem can be solved by the elastic-viscoelastic correspondence principle [30]. The stress-strain relationship is given by Laplace transform of Eq. (37),

$$\bar{\boldsymbol{\sigma}}(s) = 2s\bar{\mu}(s)\bar{\boldsymbol{\varepsilon}}(s) + s\bar{\lambda}(s)[\bar{\boldsymbol{\varepsilon}}(s):\boldsymbol{\delta}]\boldsymbol{\delta} \tag{38}$$

where a bar over a variable denotes its Laplace transformed form and s is the transform variable. The nonvanishing stress traction in Laplace transformed form is

$$\bar{N}_{33} = \frac{\bar{\beta}\cos(kx_1)}{2R}, \quad |x_2|\leq R, x_3 = 0 \tag{39}$$

Equations (38) and (39) are identical to that of linear elasticity if the transform of viscoelastic variables (e.g., $\bar{\boldsymbol{\sigma}}(s)$ and $\bar{\boldsymbol{\varepsilon}}(s)$) are associated with the corresponding elastic variables (e.g., $\boldsymbol{\sigma}$ and $\boldsymbol{\varepsilon}$) and the transformed moduli (e.g., $s\bar{\mu}(s)$ and $s\bar{\lambda}(s)$) are associated with elastic moduli μ_e and λ_e. Thus the solution of the Laplace transformed viscoelastic problem can be directly obtained from

the solution of the corresponding elastic problem by replacing μ_e and λ_e with $s\bar{\mu}(s)$ and $s\bar{\lambda}(s)$. The corresponding elastic problem for Eqs. (38) and (39) has been resolved in Sec. 4 using Kelvin's solution [27]. Then the displacement at point $\mathbf{x}=(x_1,x_2,0)$ due to a distributed load (Eq. (39)) in viscoelastic cytoplasm is obtained from the corresponding elastic solution given by Eq. (26),

$$\bar{u}_3(x_1,x_2,0,s) = \int_{-R}^{R}\int_{-\infty}^{\infty} \frac{\bar{\beta}\cos(kx_1^0)}{16\pi R s\bar{\mu}(s)} \frac{1}{\sqrt{(x_1-x_1^0)^2+(x_2-x_2^0)^2}} dx_1^0 dx_2^0$$

$$= \frac{\bar{\beta}\cos(kx_1)}{8\pi R s\bar{\mu}(s)}\{2R(1-\gamma)+2R\ln 2-(R+x_2)\ln[k(R+x_2)]-(R-x_2)\ln[k(R-x_2)]\} \tag{40}$$

The viscoelasticity of cytoplasm is specifically modeled as a Kelvin model [30], i.e., the viscoelastic system is modeled as a spring and a dashpot in parallel, and the shear relaxation modulus is

$$\mu(t) = \mu_e + \eta\delta(t) \tag{41}$$

where μ_e is the stiffness of the spring and η is the viscosity of the dashpot. The spring is used to model the elastic cytoskeleton such that μ_e is the shear modulus in Sec. 4. The dashpot models the viscous fluid and therefore η is the viscosity in Sec. 3. Here the viscoelasticity analysis involves both elasticity through shear modulus μ_e and viscosity η, and therefore exhibits profound effects on the microtubule buckling, as shown in the following.The Laplace transform of the shear relaxation modulus is

$$\bar{\mu}(s) = \frac{\mu_e}{s} + \eta \tag{42}$$

Substitute Eq. (42) into Eq. (40) and the inverse Laplace transform gives

$$\dot{u}_3(x_1,x_2,0) = -\frac{\mu_e}{\eta}u_3 + \frac{\beta\cos(kx_1)}{8\pi R\eta}\{2R(1-\gamma)+2R\ln 2-(R+x_2)\ln[k(R+x_2)]-(R-x_2)\ln[k(R-x_2)]\} \tag{43}$$

Similar to viscous analysis in Sec. 3, the viscoelastic cytoplasm is coupled with the buckled microtubule via the stress and velocity continuity condition across the interface. To be specific, the vertical velocity of the viscoelastic cytoplasm at the microtubule/cytoplasm interface (Eq. (43)) is continuous with the microtubule velocity derived from Eq. (4) on the average sense, i.e., the average velocity of the viscoelastic cytoplasm over the microtubule diameter $2R$,

$$\dot{u}_3^{\text{avg}}(x_1) = \frac{1}{2R}\int_{-R}^{R}\dot{u}_3(x_1,x_2,0)dx_2 = -\frac{\mu_e}{\eta}u_3 + \frac{\beta\cos(kx_1)}{8\pi\eta}[3-2\gamma-2\ln(kR)] \tag{44}$$

is the same as the microtubule velocity given by Eq. (4). Thus the continuity condition is

$$\frac{dA}{dt} = -\frac{\mu_e}{\eta}A + \frac{\beta}{8\pi\eta}[3-2\gamma-2\ln(kR)] \tag{45}$$

Here we only consider the initial growth of buckling from the small perturbation of A in Eq. (4) such that β is linearized (the same as Eq. (18)), and the linear ordinary differential equation for small perturbation A becomes

$$\frac{dA}{dt} = \left\{-\frac{\mu_e}{\eta} + \frac{E_{\text{MT}}I}{8\pi\eta}\left(\frac{P}{E_{\text{MT}}I}-k^2\right)[3-2\gamma-2\ln(kR)]k^2\right\}A \tag{46}$$

Compared with the differential equation of A in viscous analysis (Eq. (19)), μ_e/η comes into play in viscoelastic analysis. $\mu_e/\eta=0$ corresponds to viscous cytosol presented in Sec. 3, while

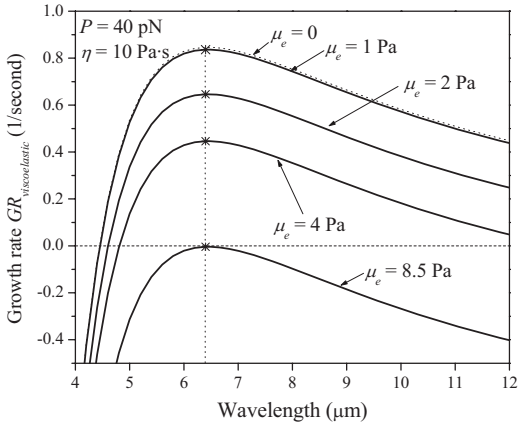

Fig. 6 The relationship of growth rate and wavelength for viscoelastic cytoplasm with different shear moduli

$\mu_e/\eta\to\infty$ denotes that the elasticity prevails in the viscoelastic cytoplasm. Let the initial amplitude be A_0, the evolution of the amplitude is

$$A = A_0\exp\left\langle\left\{-\frac{\mu_e}{\eta}+\frac{E_{\text{MT}}I}{8\pi\eta}\left(\frac{P}{E_{\text{MT}}I}-k^2\right)[3-2\gamma-2\ln(kR)]k^2\right\}t\right\rangle = A_0 e^{\text{GR}_{\text{viscoelastic}}t} \tag{47}$$

where

$$\text{GR}_{\text{viscoelastic}} = -\frac{\mu_e}{\eta}+\frac{E_{\text{MT}}I}{8\pi\eta}\left(\frac{P}{E_{\text{MT}}I}-k^2\right)[3-2\gamma-2\ln(kR)]k^2 \tag{48}$$

is the growth rate for viscoelastic cytoplasm.

The stability of the perturbed microtubules depends on the sign of the growth rate $\text{GR}_{\text{viscoelastic}}$. When $\text{GR}_{\text{viscoelastic}}>0$ for some wavelengths, the initial fluctuations associated with these wavelengths grow in an exponential law with growth rate $\text{GR}_{\text{viscoelastic}}$. While when $\text{GR}_{\text{viscoelastic}}<0$ for some wavelengths, the initial fluctuations characterized by these wavelengths decay and the microtubules are stable. The critical condition is $\text{GR}_{\text{viscoelastic}}=0$. The three stages of evolution of perturbed microtubules are shown in Fig. 6. The parameters used in Fig. 6 are bending rigidity $E_{\text{MT}}I=2\times10^{-23}$ N m^2 [10], $P=40$ pN, viscosity $\eta=10$ Pa s, and shear modulus $\mu_e=0-8.5$ Pa. Compared with Fig. 4 for viscous cytoplasm, the introduction of shear modulus has important effects.

With the increase in shear modulus μ_e from 0 (corresponding to viscous case) to finite value, the viscoelastic cytoplasm becomes more "elastic" and all of the curves shift downward but do not change shape, which leads to an increase in the critical wavelength. For example, the critical wavelength for $\mu_e=2$ Pa is 4.6 μm, while it is 4.9 μm for $\mu_e=4$ Pa. The fastest growth wavelength is determined by $\partial\text{GR}_{\text{viscoelastic}}/\partial k=0$,

$$\lambda = 2\pi\left[\frac{E_{\text{MT}}I}{P}\frac{5-4\gamma-4\ln(2\pi R/\lambda)}{3-2\gamma-2\ln(2\pi R/\lambda)}\right]^{1/2} \tag{49}$$

with an approximated expression as

$$\lambda_{\text{viscoelastic}}^{\text{fastest growth}} \approx 2\pi\sqrt{\frac{2E_{\text{MT}}I}{P}} \tag{50}$$

which is independent of shear modulus μ_e and the same as that for viscous analysis given by Eq. (24). Equation (50) suggests that once the dynamic growth occurs, the fastest growth wavelength is completely determined by the axial compressive force P and the bending rigidity $E_{\text{MT}}I$ of microtubules but does not depend on the properties of the cytoplasm (elasticity μ_e and viscosity η).

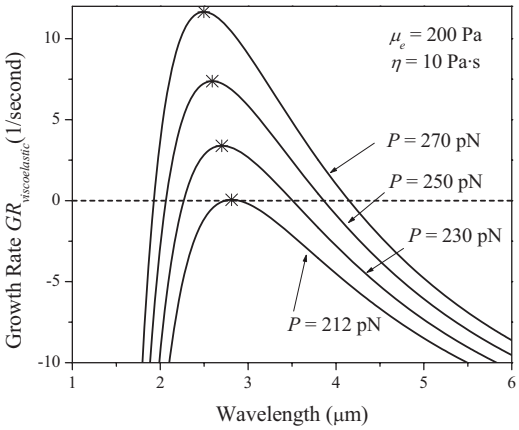

Fig. 7 The relationship of growth rate and wavelength for viscoelastic cytoplasm with different axial compressive forces

If shear modulus further increases, e.g., $\mu_e=8.5$ Pa in Fig. 6, the growth rate $GR_{viscoelastic}<0$ for all wavelengths. This suggests that the buckling is suppressed by the viscoelastic cytoplasm. The critical shear modulus μ_e^c is determined by setting $GR_{viscoelastic}=0$ and $\partial\mu_e^c/\partial k=0$, which gives

$$\mu_e^c = \frac{P^2}{32\pi E_{MT} I}\left[3-2\gamma-2\ln\left(\sqrt{\frac{P}{2EI}}R\right)\right] \tag{51}$$

For a given axial force P, cytoplasm with shear modulus larger than μ_e^c prevents the growth for all wavelengths. The elasticity of the cytoplasm allows the system the ability to block microtubule buckling, while the viscosity of the cytoplasm does not block microtubule buckling and only affects the growth rate. In Fig. 6, the growth rate $GR_{viscoelastic}$ is about 1/s, which suggests that if buckling process occurs, it occurs on the order of seconds.

Figure 7 shows the growth rate curve for different axial force P with shear modulus $\mu_e=200$ Pa and viscosity $\eta=10$ Pa s. The critical wavelength and fastest growth wavelength increase with the decrease in the axial force P. When $P=212$ pN, the growth rate is zero, which gives a critical axial compressive force $P^c_{viscoelastic}$. If the axial compressive force is less than $P^c_{viscoelastic}$, the initial perturbation will decay and the microtubule buckling does not occur. The critical force $P^c_{viscoelastic}$ is obtained by solving $GR_{viscoelastic}=0$ and $\partial P^c_{viscoelastic}/\partial k=0$,

$$P^c_{viscoelastic} = \frac{25}{16}\sqrt{E_{MT} I \mu_e}\left\{1+\frac{2048\pi}{625[3-2\gamma-2\ln(kR)]}\right\} \tag{52}$$

and the corresponding critical wavelength is

$$\lambda^c_{viscoelastic} = \frac{8\pi}{5}\left(\frac{E_{MT} I}{\mu_e}\right)^{1/4} \tag{53}$$

The critical force and wavelength are identical to that for the elastic cytoplasm, which indicates that the threshold for microtubule buckling is completely governed by cytoplasm elasticity. Therefore, the discussion of the compressive force that an individual microtubule can bear in the elastic analysis also holds here.

6 Discussion and Concluding Remarks

In this study, mechanics models for the analysis of microtubule buckling supported by cytoplasm have been reported. The microtubule is modeled as a linearly elastic cylindrical tube while the cytoplasm is characterized by viscous, elastic, or viscoelastic material. The microtubule is coupled with the cytoplasm through interface continuity conditions. The dynamic evolution equations, fastest growth rate, critical wavelength, and critical compressive force, as well as equilibrium buckling configurations are obtained.

To understand the process completely, one must not only consider the energy of deformed configuration but also the dynamics. The dynamic effect is due to the cytoplasm viscosity that affects the growth rate, while the energetic process is governed by the cytoplasm elasticity that determines the occurrence of buckling. Once the buckling occurs, the final equilibrium configuration is completely determined by the elasticity. These processes, namely, dynamic growth and elastic equilibrium, are similar for the bilayer structures that have been studied previously [31–37]. The ability of a cell to sustain compressive force is not solely determined by microtubules but also the elasticity of cytoplasm. With the support of the cytoplasm, an individual microtubule can sustain a compressive force on the order of 100 pN. The relatively stiff microtubules and compliant cytoplasm are combined to provide a scaffold for compressive force.

In addition to the mechanics explanation of microtubule buckling supported by cytoplasm, the findings in this study can be influential due to the concise analytical description of the critical force and wavelength. For example, since the bending rigidity of microtubules is well accepted on the range of 0.4×10^{-23}–4×10^{-23} N m^2, the expression for critical wavelength provides a means to measure the shear modulus of cytoplasm that is closely related to many diseases, such as cancer [38].

There exists some related works. For example, Liu et al. [39] studied the buckling of a microtubule bundle in tubulin solution. They observed a short-wavelength buckling pattern and obtained a power law for buckling wavelength $\lambda\propto R(E_{MT}/\mu_e)^{1/4}$, which is the same as the current analysis. Im and Huang [36] showed the similar relation between buckling wavelength and ratio of thin film and substrate for thin film buckling on an elastic-viscoelastic bilayer. A recent work by Das et al. [40] studied the mechanism of microtubule buckling in cells. Similar relations between buckling profiles and substrate modulus were obtained. The main difference is that the current analysis has a more quantitative mechanics analysis.

Acknowledgment

H.J. acknowledges the financial support from the Fulton School of Engineering at ASU. H.J. also acknowledges the partial support from NSF CMMI-0700440. The discussion with Professor Rui Huang in the University of Texas in Austin is also acknowledged.

References

[1] Alberts, B., Johnson, A., Lewis, J., Raff, M., Roberts, K., and Walter, P., 2003, *Molecular Biology of the Cell*, Garland Science, New York.
[2] Howard, J., and Hyman, A. A., 2003, "Dynamics and Mechanics of the Microtubule Plus End," Nature (London), **422**, pp. 753–758.
[3] Bao, G., and Suresh, S., 2003, "Cell and Molecular Mechanics of Biological Materials," Nat. Mater., **2**, pp. 715–725.
[4] Karsenti, E., Nedelec, F., and Surrey, T., 2006, "Modelling Microtubule Patterns," Nat. Cell Biol., **8**, pp. 1204–1211.
[5] Kolodney, M. S., and Wysolmerski, R. B., 1992, "Isometric Contraction by Fibroblasts and Endothelial-Cells in Tissue-Culture-A Quantitative Study," J. Cell Biol., **117**, pp. 73–82.
[6] WatermanStorer, C. M., and Salmon, E. D., 1997, "Actomyosin-Based Retrograde Flow of Microtubules in Migrating Epithelial Cells Influences Dynamic Instability and is Associated With Microtubule Breakage and Treadmilling," Mol. Biol. Cell, **8**, p. 17.
[7] Putnam, A. J., Cunningham, J. J., Dennis, R. G., Linderman, J. J., and Mooney, D. J., 1998, "Microtubule Assembly is Regulated by Externally Applied Strain in Cultured Smooth Muscle Cells," J. Cell. Sci., **111**, pp. 3379–3387.
[8] Wang, N., Naruse, K., Stamenovic, D., Fredberg, J. J., Mijailovich, S. M., Toric-Norrelykke, I. M., Polte, T., Mannix, R., and Ingber, D. E., 2001, "Mechanical Behavior in Living Cells Consistent With the Tensegrity Model," Proc. Natl. Acad. Sci. U.S.A., **98**, pp. 7765–7770.
[9] Stamenovic, D., Mijailovich, S. M., Tolic-Norrelykke, I. M., Chen, J. X., and Wang, N., 2002, "Cell Prestress. II. Contribution of Microtubules," Am. J. Physiol.: Cell Physiol., **282**, pp. C617–C624.
[10] Gittes, F., Mickey, B., Nettleton, J., and Howard, J., 1993, "Flexural Rigidity of Microtubules and Actin-Filaments Measured From Thermal Fluctuations in Shape," J. Cell Biol., **120**, pp. 923–934.
[11] Dogterom, M., and Yurke, B., 1997, "Measurement of the Force-Velocity Re-

lation for Growing Microtubules," Science, **278**, pp. 856–860.
[12] Gittes, F., Meyhofer, E., Baek, S., and Howard, J., 1996, "Directional Loading of the Kinesin Motor Molecule as it Buckles a Microtubule," Biophys. J., **70**, pp. 418–429.
[13] Brangwynne, C. P., MacKintosh, F. C., Kumar, S., Geisse, N. A., Talbot, J., Mahadevan, L., Parker, K. K., Ingber, D. E., and Weitz, D. A., 2006, "Microtubules can Bear Enhanced Compressive Loads in Living Cells Because of Lateral Reinforcement," J. Cell Biol., **173**, pp. 733–741.
[14] Timoshenko, S., and Gere, J., 1961, *Theory of Elastic Stability*, McGraw-Hill, New York.
[15] Huang, Z. Y., Hong, W., and Suo, Z., 2005, "Nonlinear Analyses of Wrinkles in a Film Bonded to a Compliant Substrate," J. Mech. Phys. Solids, **53**, pp. 2101–2118.
[16] Chen, X., and Hutchinson, J. W., 2004, "Herringbone Buckling Patterns of Compressed Thin Films on Compliant Substrates," ASME J. Appl. Mech., **71**, pp. 597–603.
[17] Berk, A., Zipursky, S. L., Matsudaira, P., David, B., and Darnell, J., 2001, *Molecular Cell Biology*, Scientific American Library, New York.
[18] Sugi, H., and Chaen, S., 2003, "Force-Velocity Relationships in Actin-Myosin Interactions Causing Cytoplasmic Streaming in Algal Cells," J. Exp. Biol., **206**, pp. 1971–1976.
[19] Chaen, S., Inoue, J., and Sugi, H., 1995, "The Force-Velocity Relationship of the Atp-Dependent Actin-Myosin Sliding Causing Cytoplasmic Streaming in Algal Cells, Studied Using a Centrifuge Microscope," J. Exp. Biol., **198**, pp. 1021–1027.
[20] Pickard, W. F., 2003, "The Role of Cytoplasmic Streaming in Symplastic Transport," Plant, Cell Environ., **26**, pp. 1–15.
[21] Pozrikidis, C., 1997, *Introduction to Theoretical and Computational Fluid Dynamics*, Oxford University Press, New York.
[22] Abramowitz, M., and Stegun, I. A., 1972, *Handbook of Mathematical Functions With Formulas, Graphs, and Mathematical Tables*, Dover, New York.
[23] Fushimi, K., and Verkman, A. S., 1991, "Low Viscosity in the Aqueous Domain of Cell Cytoplasm Measured by Picosecond Polarization Microfluorimetry," J. Cell Biol., **112**, pp. 719–725.
[24] Swaminathan, R., Hoang, C. P., and Verkman, A. S., 1997, "Photobleaching Recovery and Anisotropy Decay of Green Fluorescent Protein GFP-S65T in Solution and Cells: Cytoplasmic Viscosity Probed by Green Fluorescent Protein Translational and Rotational Diffusion," Biophys. J., **72**, pp. 1900–1907.
[25] Bicknese, S., Periasamy, N., Shohet, S. B., and Verkman, A. S., 1993, "Cytoplasmic Viscosity Near the Cell Plasma-Membrane-Measurement by Evanescent Field Frequency-Domain Microfluorimetry," Biophys. J., **65**, pp. 1272–1282.
[26] Mofrad, M. R. K., and Kamm, R. D., 2006, *Cytoskeletal Mechanics: Models and Measurements*, Cambridge University Press, Cambridge.
[27] Kachanov, M., Shafiro, B., and Tsukrov, I., 2003, *Handbook of Elasticity Solutions*, Kluwer Academic, Boston.
[28] Canetta, E., Duperray, A., Leyrat, A., and Verdier, C., 2005, "Measuring Cell Viscoelastic Properties Using a Force-spectrometer: Influence of Protein-Cytoplasm Interactions," Biorheology, **42**, pp. 321–333.
[29] Kasza, K. E., Rowat, A. C., Liu, J. Y., Angelini, T. E., Brangwynne, C. P., Koenderink, G. H., and Weitz, D. A., 2007, "The Cell as a Material," Curr. Opin. Cell Biol., **19**, pp. 101–107.
[30] Christensen, R. M., 1971, *Theory of Viscoelasticity: An Introduction*, Academic, New York.
[31] Huang, R., 2005, "Kinetic Wrinkling of an Elastic Film on a Viscoelastic Substrate," J. Mech. Phys. Solids, **53**, pp. 63–89.
[32] Huang, R., and Im, S. H., 2006, "Dynamics of Wrinkle Growth and Coarsening in Stressed Thin Films," Phys. Rev. E, **74**, p. 026214.
[33] Huang, R., and Suo, Z., 2002, "Wrinkling of a Compressed Elastic Film on a Viscous Layer," J. Appl. Phys., **91**, pp. 1135–1142.
[34] Huang, R., and Suo, Z., 2002, "Instability of a Compressed Elastic Film on a Viscous Layer," Int. J. Solids Struct., **39**, pp. 1791–1802.
[35] Huang, Z. Y., Hong, W., and Suo, Z., 2004, "Evolution of Wrinkles in Hard Films on Soft Substrates," Phys. Rev. E, **70**, p. 030601.
[36] Im, S. H., and Huang, R., 2005, "Evolution of Wrinkles in Elastic-viscoelastic Bilayer Thin Films," ASME J. Appl. Mech., **72**, pp. 955–961.
[37] Jiang, H., Khang, D.-Y., Song, J., Sun, Y., Huang, Y., and Rogesr, J. A., 2007, "Finite Deformation Mechanics in Buckled Thin Films on Compliant Supports," Proc. Natl. Acad. Sci. U.S.A., **104**, pp. 15607–15612.
[38] Suresh, S., 2007, "Biomechanics and Biophysics of Cancer Cells," Acta Mater., **55**, pp. 3989–4014.
[39] Liu, Y. F., Guo, Y. X., Valles, J. M., and Tang, J. X., 2006, "Microtubule Bundling and Nested Buckling Drive Stripe Formation in Polymerizing Tubulin Solutions," Proc. Natl. Acad. Sci. U.S.A., **103**, pp. 10654–10659.
[40] Das, M., Levine, A. J., and MacKinstosh, F. C., 2008, "Buckling and Force Propagation Along Intracellular Microtubules," e-print arXiv:0709.2344.